Digest Journal of Nanomaterials and Biostructures Vol. 10, No. 3, July - September 2015, p. 823 - 830

ENHANCED PHOTOCATALYTIC OF ZnO NANOSTRUCTURES VIA SHAPE CONTROLLED PLATINUM THIN FILM

M. RASHAD[a,b] N. M. SHAALAN[a*], M. M. HAFIZ[a]
[a]*Physics Department, Faculty of Science, Assiut University,71516 Assiut, Egypt*
[b]*Physics Department, Faculty of Science, University of Tabuk, P.O. Box 741, Tabuk, 71491, KSA*

Various nanostructures of zinc oxide (ZnO) were prepared on bare and functioned silicon substrates by developed thermal evaporation method. The nanostructures have been controlled by the functionalization of the substrate surface, where polished silicon was functionalized with Pt-template and Pt-film on its surface. The samples were characterized by field emission scanning electron microscopy, X-ray diffarctometer, and UV-vis absorbance spectra. As a variation of the substrate surface, the ZnO product showed different surface morphologies of nanostructures. X-ray data has confirmed the purity of ZnO and the impurities of Pt in the samples deposited on functionalized substrates. The photocatalytic activity of ZnO nanostructures in a wastewater was investigated by the degradation of methylene blue. Photocatalytic activity was enhanced by using Pt functionalization, and the best photocatalytic performance was recorded for the ZnO/Pt-film/Si sample.

(Received May 9, 2015; Accepted July 22, 2015)

Keywords: Nanostructures, oxides, electron microscopy, optical properties

1. Introduction

The semiconductor photocatalytic process has recently received a great attention as environmental friendly, low cost, and sustainable treatment technology in the wastewater industry. The ability of this advanced oxidation technology has been widely established to remove persistent organic compounds and microorganisms in water [1, 2]. As it is known that the reaction basically occurs on the surface of photocatalytic layer and an increase in the active surface area of the oxide would enhance and improve its properties. One-dimensional (1D) semiconductor nanostructures are focal spot of researchers because of their application in electronics, optoelectronics, and sensor devices on the nanometer scale. They possess novel properties intrinsically associated with low dimensionality and size confinement [3-5]. There is a considerable interest of metal oxide materials, especially zinc oxide (ZnO) as one of the most promising n-type semiconductor materials. One-dimensional ZnO nanorods are generated in the reaction mixture by heterogeneous nucleation and growth along the [0001] direction of the ZnO crystal [6]. ZnO thin films have been applied as gas sensors [7], light-emitting diodes [8], field emission devices [9], solar cells [10], and environmental protection [11]. In addition, it has been used in various medical drugs. Several chemicals and physical methods, such as sol–gel [12], spray pyrolysis [13], chemical vapor deposition [14], and sputtering [15] have been used to prepare ZnO films. Recently, several studies have been performed on the synthesis of ZnO nanorods, via a two step process, including the deposition of a crystal seed layer/film on the substrates and subsequent aqueous chemical growth, in which the pre-obtained precursor ZnO film would have some effect on the morphology and the size of the ZnO nanostructures. In this study, crystalline ZnO nanorods were synthesized on silicon

*Corresponding author: nshaalan@aun.edu.eg

substrate functionalized with and without Pt through the thermal evaporation method at temperature of 900°C under ambient pressure. The influence of shape-controlled platinum on the crystal growth and morphology of ZnO was discussed. The photocatalytic performance of ZnO nanostructures on degradation of methylene blue (MB) in the wastewater was carried out.

2. Material and methods

2.1 Preparations of ZnO nanomaterials

The deposition of ZnO was carried out by a thermal evaporation method, which outlined in Fig. 1a. First, commercially available ZnO powders of 10 mg with purity higher than 99.99% were placed in a small alumina crucible which was covered by a silicon substrate. The chamber was evacuated using a rotary vacuum pump to 0.8 Torr of ambient air. The crucible was then heated from room temperature (RT) to 900°C within three minutes and maintained at this temperature for one hour. At the end of the deposition the crucible was cooled to RT under the same pressure, leading to a substrate surface coated with a thick layer of ZnO products. The products of ZnO were synthesized on Si substrates; bare, functionalized with 50 nm Pt-template, and functionalized with 50 nm Pt-film, as shown in Figs. 1b-1c. Both Pt-template and Pt-film was deposited on silicon by using a DC-magnetron sputtering technique.

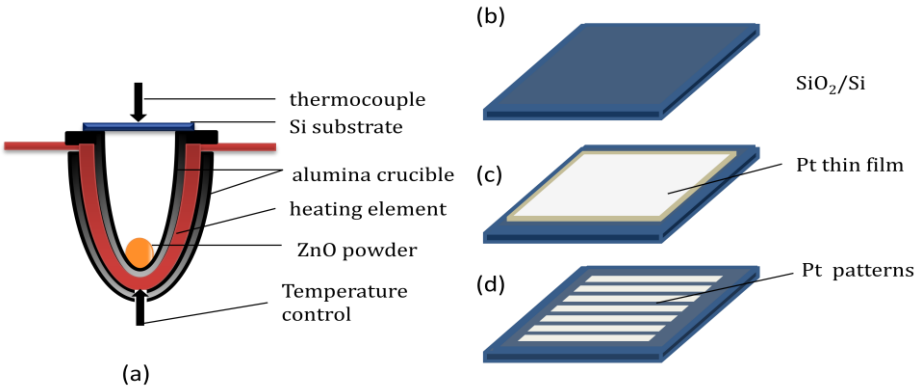

Fig. 1: Conventional thermal evaporation system (a), bare and functionalized silicon substrates (b-d).

2.2 Characterization of ZnO nanomaterials

The surface morphologies of ZnO nanostructures were characterized by field-emission scanning electron microscopy (FESEM) (JEOL, FE-SEM 6700) with accelerated voltage of 5 keV. The crystalline structures of the ZnO samples were characterized by X-ray diffraction (XRD) using a diffractometer with Cu Kα radiation (Shimadzu XRD-6100), λ= 0.154 nm in the range of 2θ = 20–65°, with scan rate of 2°/min. The UV–visible absorbance spectra of the ZnO samples were measured using Lambda 750 UV–vis spectrophotometer with a scanning rate of 5 nm/s.

2.3 Photocatalysis measurements

The photocatalytic activities of the ZnO samples were estimated by the degradation of MB of 1×10^{-6} M in a pyrex reactor by using an artificial sunlight simulator of 100 mW/cm^2 (model: Oriel SO12A Solar Simulators) with an ultraviolet filter, as shown in Fig. 2. The degradation of MB in the water due to the photocatalytic reactions were determined by monitoring the changes of the main absorbance peak at a wavelength of 664 nm.

Fig. 2: Sun simulator system (model: Oriel SO12A Solar Simulators)

3. Results and discussions

3.1 Microstructure characteristics

In order to understand the phase symmetry of the prepared ZnO, a systematic study on the XRD was performed. Fig.3 shows the XRD patterns of ZnO deposited at 0.8 Torr and 900°C for one hour on: bare silicon substrate, 50 nm Pt-template/Si substrate, and 50 nm Pt–film/Si substrate. It can be seen that all the peaks of samples are in a good agreement with a hexagonal structure of ZnO (ICSD card No. 36-1451). Clear and sharp diffraction peaks reveal that the deposited ZnO film is of a high crystalline quality. Sharp peaks were obtained at angles corresponding to the planes of (100), (002), (101), (102), (110) and (103). It is clearly observed that the crystal structure is dependent on the functionalization of substrate, while the preferred orientation does not change. No characteristic peaks are observed for any other impurities expect the peaks of Pt for both samples **b** and **c** which identified by ICSD cards No. 87-0647 and No. 87-0646, respectively. The (111) and (200) Pt peaks are slightly observed in the sample of Pt-template while it is clearly seen in the sample of Pt-film. Fig. 3b displays that there is 0.6° shift in (111) diffraction peak of ZnO/Pt-film and ZnO/Pt-template. This proved that Pt incorporation led to lattice deformation in the doped ZnO and formed its crystal. All of these observations indicate that Pt entered the crystal lattice of ZnO nanostructure without deteriorating the original crystal structure. ZnO nanostructures were observed by using FESEM, confirming that ZnO is a wealthy material by creating nanostructure shapes. The low and high-magnification SEM images shown in Fig. 4 revealed that the products were significantly affected by using Pt as catalyst with different shapes (film or fingers-like template). One may observe a considerable diversity in geometric parameters of 1D structure. For pure ZnO, the SEM images show that the product consists of rods-like structure with a smooth surface. Each rod has a height of 400 nm and a diameter of 100 nm, and the hexagonal shape is clearly seen at the tip of rods, as shown in Fig. 4a. At the tip of some rods, the wire-like needle is observed with a length of 500 nm. The morphology of the pattern is changed when the substrate was coated by Pt fingers-like template; the gap width is 50 μm. When the ZnO was deposited, ZnO nanostructure was grown exclusively on the surface of Pt, leaving the gap approximately empty, as shown in Fig .4b. Although the conditions of deposition are permanent throughout the experiment except the change in substrate surface, the morphology is largely dependent on the profile of Pt material. Nanowires-like ribbons are grown with a length of 5-10 μm, a width of 200 nm and thickness of 50 nm. Needles-like wire with two stepladders are observed at the tip of formed nanowires. In case of Pt film, ZnO nanowires of 15-20 μm in length and 400 nm in diameter were grown, as shown in Fig.4c. The nanowires are decorated with particles on their surface randomly oriented and grown parallel to the substrate surface.

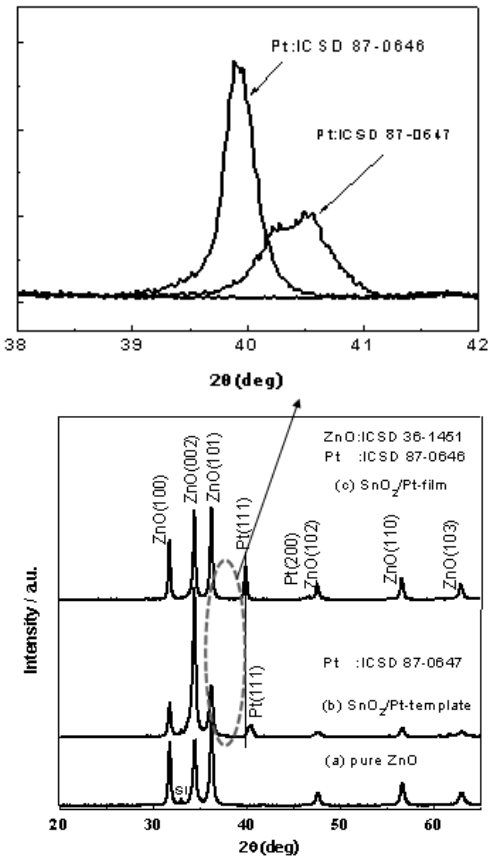

Fig. 3: XRD charts of ZnO samples: bare silicon substrate (a), 50 nm Pt-template functionalized substrate (b), and 50 nm Pt thin film-coated substrate (c).

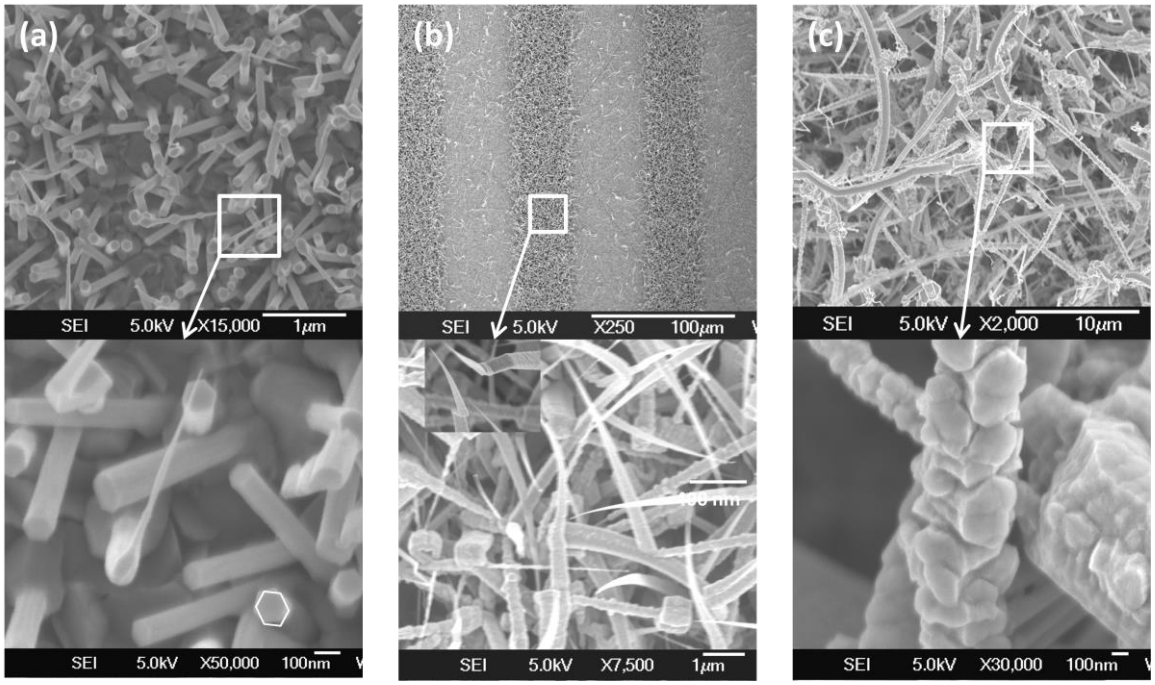

Fig. 4: FE-SEM image of ZnO samples: bare silicon substrate (a), 50 nm Pt-template functionalized substrate (b), and 50 nm Pt thin film-coated substrate (c).

3.2 Mechanism of ZnO synthesis

In the present method, we consider the growth of ZnO nanomaterials using vapor pressure as follows. The substrate temperature greatly influences the growth of the nanostructure formed by thermal evaporation method [16]. Firstly, the atoms or molecules arrive at the heated substrate and adsorb on the surface. The heating during deposition causes the surface atoms just landed not to be frozen-in at their landing sites, but diffuse by the available thermal energy. Secondly, ZnO molecules are aggregated on the surface, where the surface adatom mobility occurs in each atomic layer during the deposition and it is dictated by the heating during the deposition. In other words, the adsorbed species react with each other and also with the substrate surface, establishing the bases or nuclei for building up the ZnO nanostructures. With continuous adsorption of ZnO molecules, one-dimensional nanostructure could be formed, as shown in Fig. 4. Due to the non-epitaxial relation with SiO_2, every nucleus forms one single nanorod, and then these nanorods grow on the substrate randomly. In case of bare and Pt-functionalized silicon substrate the thermal energy is uniformly distributed on the surface, whereas, it is unceremoniously distributed in case of Pt-template because the surface of the substrate is not fully coated by Pt. Because of mentioned reason, the ZnO nanomaterials have preferred to grow up on Pt fingers, evading from the exposed surface of SiO_2.

3.3 Photocatalysis characteristics

Photocatalytic activity of ZnO nanostructures for water treatment is studied. MB is commonly considered as a representative organic dye in textile effluents, and it can easily be monitored by optical absorption spectroscopy [17]. MB is chosen as model contaminants to evaluate the photocatalytic activities of the ZnO samples due to its stability under visible light irradiation. The concentrations of MB during the photocatalytic reactions were determined by monitoring the changes of the main absorbance maximized at 664 nm.

Fig. 5a showed the absorbance variation of MB solution during the photocatalytic degradation experiments on ZnO deposited on bare Si substrate, and the MB solution turned approximately colorless within 120 min of irradiation. Similar experiments were carried out for other samples of ZnO deposited on Pt–template/Si and Pt-film/Si substrates. The spectra are shown in Figs.5b and 5c. The variation in concentration of MB solution is plotted with irradiation time in Fig. 6. As observed from Fig. 6, the ZnO deposited on Pt-film/Si exhibited a significantly higher photocatalytic activity as comparing with that of other samples.

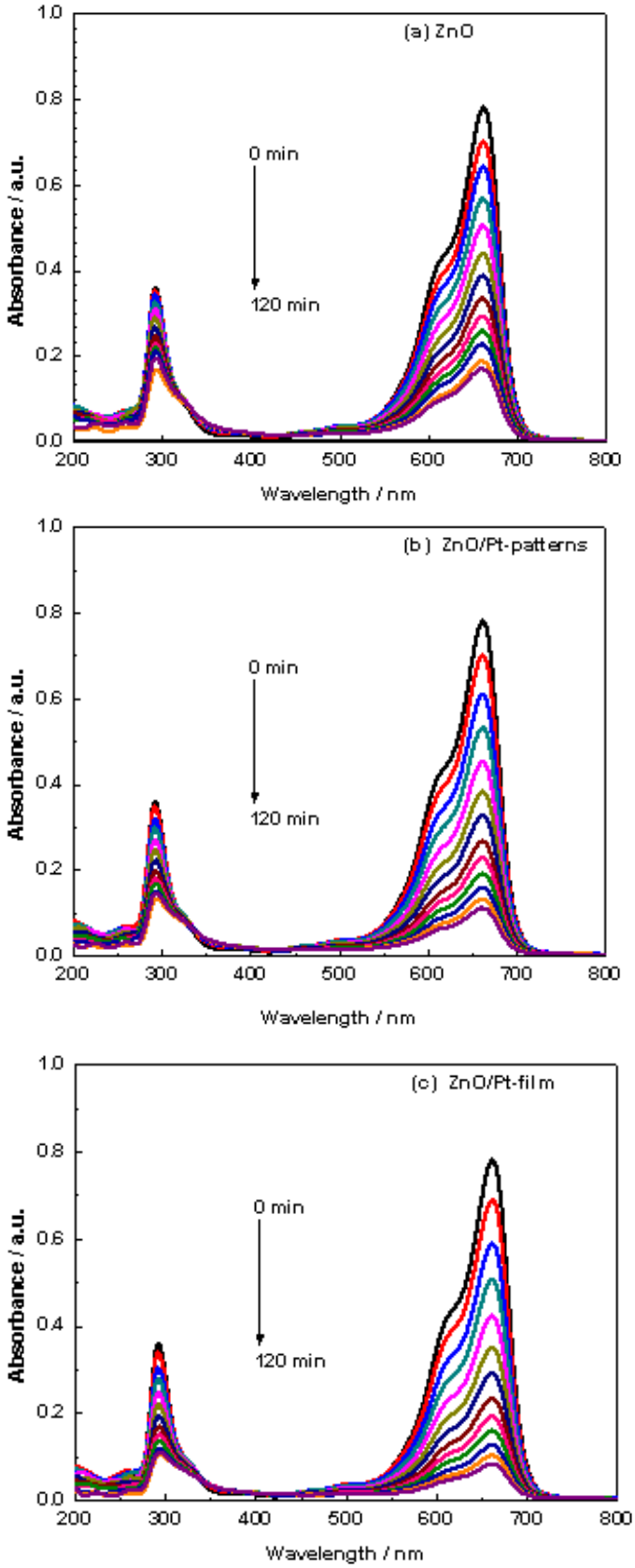

Fig. 5. Photocatalysis charts of ZnO samples: bare silicon substrate (a), 50 nm Pt-template functionalized substrate (b), and 50 nm Pt thin film-coated substrate (c).

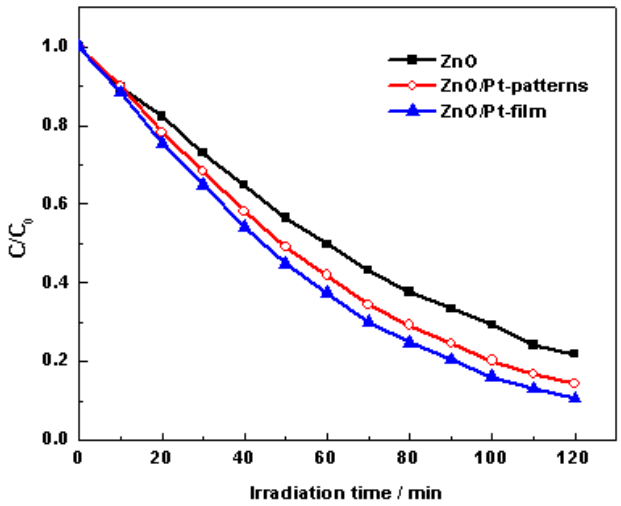

Fig. 6: Photocatalytic degradation of methylene blue (MB) on ZnO indicated by the concentration (C_0 is the initial concentration, and C is the concentration at any time) of MB with time under visible light irradiation.

The photo decolorization of MB in the presence UV light radiation is thought to be a pseudo first-order kinetic reaction. The semi-logarithmic relationship of the concentration of MB versus irradiation time yields a straight line, indicating a pseudo first order reaction [18], as shown in Fig. 7. The apparent first-order reaction rate constants (k) were evaluated from experimental data using a linear regression. The inset figure shows the dependence of the first-order reaction rate constants (k) on the irradiation time. ZnO under irradiation of light with wavelengths less than 390 nm produces electron-hole (e-h) pairs [18]. The recombination of e-h pairs reduces the rate of photocatalytic degradation of catalytic material. The positive effect of Pt on the photoactivity of ZnO at the degradation of MB may be explained by its ability to trap electrons, where Pt film is able to trap more electrons. Consequently, this process reduces the recombination of light generated e-h at ZnO surface [19]. Therefore a more effective electron transfer occurs to the acceptors and donors adsorbed on the surface of the crystals of ZnO. Oxygen adsorbed on photocatalyst surface traps the electrons and produces superoxide anion [20]. On the other hand, the holes at the ZnO surface can oxidize adsorbed water or hydroxide ions to produce hydroxyl radicals [21]. Thus, ZnO deposited on Pt-film/Si substrate sample showed the best photocatalytic performance.

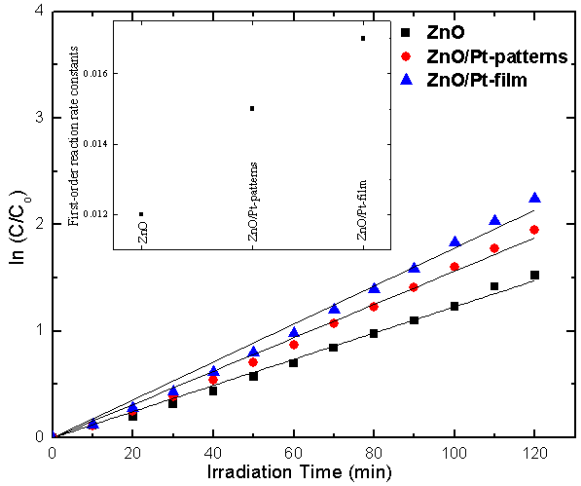

Fig. 7. Semi-logarithmic graph of MB concentration vs. irradiation time in the presence of ZnO.

4. Conclusions

Morphology-controlled ZnO nanostructures (nanorods, nanowires, and nanowire-like ribbons) have been synthesized by a developed thermal evaporation method. The surface morphologies of ZnO were controlled by functionalization the surface of the silicon substrate, and three samples were synthesized; (I) on bare Si, (II) on Pt-template/Si, and (III) on Pt-film/Si substrates. In case of Pt-template/Si, the ZnO nanostructure was grown in the places which Pt is exist and left the surface of SiO_2 between fingers relatively empty. The photocatalytic activities depended on the surface morphology, crystallinity, and Pt impurity in the sample. The photocatalytic activity of ZnO was enhanced by using Pt impurities, and the sample of ZnO/Pt-film showed the best photocatalytic performance among all samples. The photocatalytic activities of ZnO depended on the different surface morphologies. The water turned almost colorless after 120 minutes, and the ZnO/Pt-film exhibited the fast degradation of MB on its surface.

Acknowledgement

The authors would like deeply to thank Prof. Toshinari Yamazaki, University of Toyama, Japan for his helpful discussion and FE-SEM observations.

References

[1] M. N. Chong, B. Jin, C.W.K. Chow, C. Saint, Water Research **44**, 2997 (2010).
[2] I. El Saliby, L. Erdei, J.-H. Kim, H. K. Shon, Water Research **47,** 4115 (2013).
[3] W. Liu, C.M. Lieber, J. Phys. D: Appl. Phys, **39,** R387 (2006).
[4] Y. Li, F. Qian, J. Xiang, C.M. Lieber, Mater. Today **9**, 18 (2006).
[5] D. H. Zhang, Y.Y. Wang, Mater. Sci. Eng. B **134**, 9 (2006).
[6] R. Majithia, S. Ritter, K.E. Meissnera, Anal. Chim. Acta **812,** 206 (2014).
[7] Y. Abdi, S.M. Jebreiil Khadem, P. Afzali, Curr. Appl. Phys. **14**, 227 (2014).
[8] X. Mo, G. Fang, H. Long, S. Li, H. Huang, H. Wang, Y. Liu, X. Meng, Y. Zhang, C. Pan, J. Luminesce **137,** 116 (2013).
[9] F. Jamali-Sheini, R. Yousefi, D. S. Joag, M. A. More, Vacuum **101,** 233 (2014).
[10] J. Xu, K. Fan, W. Shi, K. Li, T. Peng, Solar Energy **101**, 150 (2014).
[11] G. Broasca, G. Borcia, N. Dumitrascu, N. Vrinceanu, Appl. Surf. Sci. **279,** 272 (2013).
[12] Y.F. Makableh, R. Vasan, J.C. Sarker, A.I. Nusir, S. Seal, M.O. Manasreh, Solar Energy Mater. Solar Cells **123,** 178 (2014).
[13] Y-J. Noh, S.-I. Na, S.-S. Kim, Solar Energy Materials and Solar Cells **117**, 139 (2013).
[14] A. Mohanta, J. G. Simmons, H. O. Everitt, G. Shen, S. M. Kim, P. Kung, J. Luminescence **146,** 470 (2014).
[15] J.W. Lee, K.N. Hui, K.S. Hui, Y.R. Cho, H.-H. Chun, Appl. Surf. Sci. **293,** 55 (2014).
[16] N.M. Shaalan, T. Yamazakia, T. Kikuta, Mater. Chem. Phys. **127,** 143 (2011).
[17] Z. Zhang, Md. Faruk Hossain, T. Takahashi, Mater. Letters **64,** 435 (2010).
[18] M.A. Behnajady, N.Modirshahla, M. Shokri, B. Rad, Global NEST J. **10, 1** (2008).
[19] H.M. Coleman, K. Chiang, R. Amal, Chem. Eng. J **113**, 65 (2005).
[20] N. Daneshvar, M. Rabbani, N. Modirshahla, M. A. Behnajady, J Photochem. Photobiol. A **168,** 39 (2004) .
[21] M. A. Behnajady, N. Modirshahla, N. Daneshvar, M. Rabbani, Chem. Eng. J **127,** 167 (2007).